



Research article

Antiviral Activities of Compounds Derived from Medicinal Plants against SARS-CoV-2 Based on Molecular Docking of Proteases

Mohamed Chebaibi ^{a*}, Ibrahim Mssillou ^b, Aimad Allali ^c, Mohammed Bourhia ^d, Dalila Boustia ^e, Rene Francisco Boschi Gonçalves ^f, Hasnae Hoummami ^g, Mourad A. M. Aboul-Soud ^h, Maria Augustyniak ⁱ, John P. Giesy ^j, Sanae Achour ^g

^a Ministry of Health and Social Protection, Higher Institute of Nursing Professions and Health Techniques, Fez, Morocco

^b Laboratory of Natural Substances, Pharmacology, Environment, Modeling, Health & Quality of Life (SNAMOPEQ), Faculty of Sciences Dhar El Mahraz, Sidi Mohamed Ben Abdellah University, Fez 30000, Morocco

^c Ministry of Health and Social Protection, Higher Institute of Nursing Professions and Health Techniques, Fez, Taza annex, Morocco

^d Department of Chemistry and Biochemistry, Faculty of Medicine and Pharmacy, Ibn Zohr University, Laayoune, Morocco

^e Laboratory of Neuroendocrinology and Nutritional and Climatic Environment, FSDM, University of Sidi Mohamed Ben Abdellah, Fez, Morocco

^f Aeronautics Institute of Technology Praça Marechal Eduardo Gomes, 50 São José dos Campos/SP Brazil Zip Code: 12228-900

^g Biomedical and Translational Research Laboratory, Faculty of Medicine and Pharmacy of the Fez, University of Sidi Mohamed Ben Abdellah, Fez 30000, Morocco

^h Department of Clinical Laboratory Sciences, College of Applied Medical Sciences, King Saud University, P.O. Box 10219, Riyadh 11433, Saudi Arabia.

ⁱ Institute of Biology, Biotechnology and Environmental Protection, Faculty of Natural Sciences, University of Silesia in Katowice, Bankowa 9, 40-007 Katowice, Poland

^j Toxicology Centre, University of Saskatchewan, Saskatoon, SK S7N 5B3, Canada

*Corresponding author: Mohamed Chebaibi (mohamed.chebaibi@usmba.ac.ma)

Abstract

This study aimed to evaluate the inhibitory effects of key polyphenols and flavonoids from *Syzygium aromaticum* and *Citrus limon*, along with main organosulfur compounds from *Allium sativum*, against SARS-CoV-2 proteases 6LU7 and 6Y2E. The methods used included *in silico* molecular docking, ADMET analysis, and molecular dynamics simulations. Structures of 34 natural products found in three medicinal plants were docked to these two critical proteins. For 6LU7 protease, 24 compounds exhibited binding affinities greater than or equal to -6 Kcal/mol. While, for 6Y2E protease, 6 compounds exhibited binding affinities greater than or equal to -6 Kcal/mol. Molecules with a maximum binding affinity equal to -8.4 kcal/mol show good hydrogen bonds with the two proteases under investigation, 6LU7 and 6Y2E. The ADME properties of ellagic acid, kaempferol, and biflorin showed human oral absorption rates of 43.6%, 67.5%, and 44.8% respectively, and Caco-2 permeability values of 33.429, 163.1, and 187.9 nm/s. Blood-brain partition coefficients indicate biflorin is within the acceptable range (-3 to 1.2), while ellagic acid and kaempferol exceed acceptable values (>1.2). The molecular dynamics simulation study demonstrates the rigidity and stability of the docked complexes, evidenced by substantial energy reductions indicating system stabilization. Hesperidin binds more rapidly to 6LU7 than to 6Y2E, while diosmin displayed the quickest kinetics with 6Y2E. These compounds might be used therapeutically as complementary medicines and/or to conceptualize new drugs against COVID-19.

Keywords: COVID-19; 6LU7 protease; 6Y2E protease; plants; computational virtual screening; MD simulation

Citation: Chebaibi, M.; Mssillou, I.; Allali, A.; Bourhia, M.; Boustia, D.; Gonçalves, R.F.B.; Hoummami, H.; Aboul-Soud, M. A. M.; Augustyniak, M.; Giesy, J.P.; Achour, S. Antiviral Activities of Compounds Derived from Medicinal Plants against SARS-CoV-2 Based on Molecular Docking of Proteases. *Journal of Biology and Biomedical Research*. 2024, 1, 10-30. <https://doi.org/10.69998/j2br1>

Edited by: Tarik Moubchir

1. Introduction

On May 27, 2020, the World Health Organization (WHO) declared the severe acute respiratory syndrome (SARS) of

the current coronavirus Disease 19 (COVID-19) outbreak, emerging in China at the end of 2019, as a pandemic. Since

Received: 06 April 2024; Revised: 20 May 2024; Accepted: 29 July 2024; Published: 30 July 2024

Copyright: © 2024 by the authors. Submitted for possible open access publication under the terms and conditions of the Creative Commons Attribution (CC BY) license (<https://creativecommons.org/licenses/by-nc-nd/4.0/>).

<https://fmjpublishing.com/index.php/J2BR>

then, more than 334,186,670 confirmed cases of COVID-19, including 5,570,713 deaths worldwide, have been recorded, according to the website <https://www.worldometers.info/coronavirus/>, accessed on January 19, 2022 (Mercatelli et al., 2021). Alpha-, Beta-, Gamma-, and Delta-coronaviruses are the four genera that make up the Coronaviridae family, with Alpha and Beta-coronaviruses being the human pathogens. The virus that causes COVID-19, SARS-CoV-2, also known as 2019-nCoV and severe acute respiratory syndrome (SARS) coronavirus (CoV)-2 virus, belongs to the genus Beta-coronavirus of the Coronaviridae family (Bourhia et al., 2020).

SARS-CoV-2 is similar to other members of the coronaviruses group in that it is classified as an enclosed single-stranded positive-sense RNA virus. In the lifecycle of SARS-CoV-2 viruses, the main viral proteinase (Mpro, also called 3 chymotrypsin-like protease, 3CLpro) plays an essential role in the replication of viral particles (ul Qamar et al., 2020), whereas papain-like protease (PLpro) is an essential enzyme of coronaviruses, that is required for processing viral polyproteins to generate a functional replicase complex and enable transmission of the virus (Shin et al., 2020). Immediately after SARS-CoV-2 RNA enters the host cell, the translation of viral proteins begins using the host's ribosomes. In the first step, the two polypeptides ppla and pplab are synthesized, which are then cleaved into smaller non-structural proteins. As a result of the cleavage of the polypeptides by papain-like protease, proteins are produced that interfere with host cell protein synthesis and modify the cell survival signaling pathway. The 3CLpro protease cleaves the peptides in 11 places, which leads to the release of 12 functional proteins that create conditions for the proliferation of the virus and the creation of double-membrane vesicles containing a replication and transcription complex that participates in the synthesis of new viruses (Eriani and Martin, 2022; Nakagawa et al., 2016; Pizzato et al., 2022; Wong and Saier Jr, 2021; Zhang et al., 2022). Since 3CLpro is a primary proteinase enzyme that controls the coronavirus replication complex, it represents an attractive target for therapy. If this enzyme is inhibited, replication of the virus can be minimized, and transmission can be limited. Thus, any chemicals that can inhibit 3CLpro could be prophylactic against SARS-CoV-2. Amid the race to achieve herd immunity through mass immunization programs and the pressing demand to develop effective anti-COVID-19 treatments, several pharmaceutical drugs have been repurposed to treat COVID-19, including hydroxychloroquine, lopinavir, ritonavir, darunavir, umifenovir, remdesivir, favipiravir (Costanzo et al., 2020). Recently, Pfizer's Paxlovid, made up of both nirmatrelvir and ritonavir and oral tablets, has been granted an emergency use authorization (EUA), by the U.S. Food and Drug Administration (USFDA), for the treatment of COVID-19 in both adults and children. However, to be effective, these compounds would need to be taken at relatively great

continuous doses. Therefore, they could have inherent toxic potencies. For this reason, natural products from medicinal plants hold promise (Bourhia et al., 2020; Vicidomini et al., 2021).

Since the beginning of the COVID-19 outbreak, traditional herbal remedies have been employed. Notably, 90 percent of 214 patients treated in China recovered after using some traditional treatments. Moreover, natural remedies based on honey, seed oil of black cumin (*Nigella sativa*), and flowers and buds of chamomile (*Anthemis hyaline*) have been reported to be effective for COVID-19 treatment in the Middle Eastern countries Egypt and Saudi Arabia. In Africa, represented by the Democratic Republic of Congo, a remedy is made up of clove (*Syzygium aromaticum*), blue gum (*Eucalyptus globulus*), lemon grass (*Cymbopogon citratus*), and ginger (*Zingiber officinale*). Other medicinal plants are currently utilized, under the name Covalyse®, as a preventative protocol for COVID-19 (Kanyinda, 2020). During this pandemic, the Moroccan population employed several medicinal plants as *Syzygium aromaticum*, *Citrus limon*, and *Allium sativum* to treat or prevent infection. The frequent use of plants without documentation of their effectiveness against the effects of COVID-19 is justified by cultural and economic reasons, and their general pharmacological activity is scientifically proven (Chebaibi et al., 2022). Unlike synthetic drugs, natural remedies are characterized by a broad safety margin. For example, clove oil and buds have been approved as safe food supplements by the USFDA, with an established WHO acceptable daily uptake of 2.5 mg/kg body weight in humans (Vijayasteltar et al., 2016). In India, black pepper, cinnamon, basil, and garlic have been reported as one of the most commonly employed spices to control COVID-19 spread (Singh et al., 2021). In the North-Western parts of Morocco, herbal remedies, including clove, have been reported to be frequently recommended by herbalists to treat and prevent COVID-19 (Chaachouay et al., 2021). When medicinal plants used by the Moroccan population to treat or prevent COVID-19 were cataloged, it was found that three plants, garlic, *Citrus limon*, and clove, were used more than any others. Due to several bioactive molecules, including allicin, diallyl trisulfide, and ajoene, garlic is used to treat viral infections. Antiviral effects have been demonstrated for extracts of garlic against rhinovirus, HIV, herpes simplex virus (HSV) 1 and 2 (Tsai et al., 1985; Weber et al., 1992), influenza A and B (Fenwick and Hanley, 1985), cytomegalovirus, viral pneumonia and rotavirus (Fenwick and Hanley, 1985). *Citrus limon*, another plant used to prevent COVID-19 by people in Morocco, is rich in flavonoids, such as diosmin, eriocitrin, and hesperidin. These flavonoids have several biological activities, including antiviral potencies (Del Río et al., 2004). Anti-HSV potencies of eugenin and eugenol, extracted from clove, have been reported to primarily take place through inhibition of the virus DNA polymerase leading to the block of DNA synthesis (Aboubakr et al., 2016; Cortés-Rojas et al.,

2014). Eugeniiin has also been reported to exhibit potent inhibitory activity against proteases of Dengue virus (DENV), a single-stranded positive-sense RNA virus, thereby blocking the cycle of viral replication; hence, it has been recommended as a potential natural anti-DENV therapeutic drug (Saleem et al., 2019).

Despite the effectiveness of herbal medicines against COVID-19, the molecular mechanisms, thereby their phytoconstituents interact with cognate SARS-CoV-2 targets, remain largely undetermined. In this context, since its first introduction in the 1980s, molecular docking has become one of the most fundamental and crucial *in silico* approaches for drug discovery (Aanouz et al., 2021). The recent innovative technological breakthroughs in computer sciences and the facilitated accessibility to protein structures and small molecules have aided the development of new methodologies, making docking increasingly popular in both industrial and academic contexts. Several studies have employed molecular docking analysis to predict binding affinities to examine the inhibitory effects of natural, bioactive molecules on the RBD domain of the spike protein PLpro and 3CLpro (Aanouz et al., 2021; Khaerunnisa et al., 2020; Mousavi et al., 2021; ul Qamar et al., 2020).

The objective of this study was to use structure-activity relationships to evaluate the inhibitory effects of several prevalent polyphenols and flavonoids of *Syzygium aromaticum* and *Citrus limon* as well as primary organosulfur compounds of *Allium sativum* against COVID-19 6LU7 and 6Y2E proteases, predicted by *in silico*

molecular docking, ADMET analysis, and molecular dynamics simulations.

2. Materials and Methods

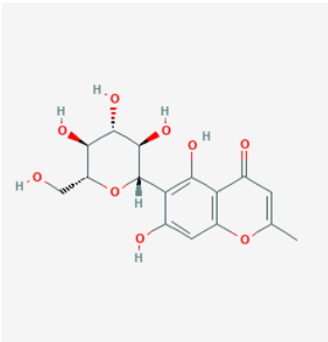
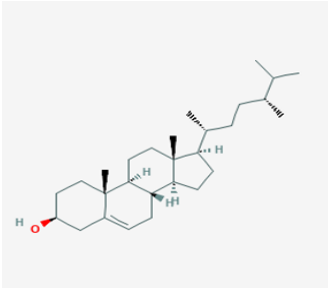
2.1. Data sets

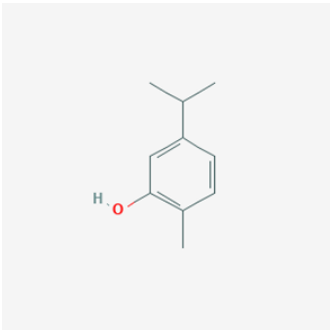
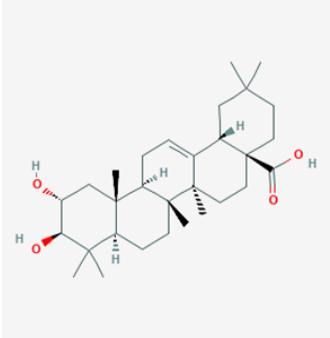
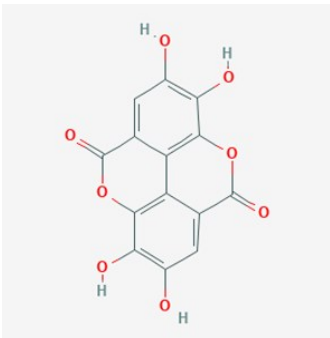
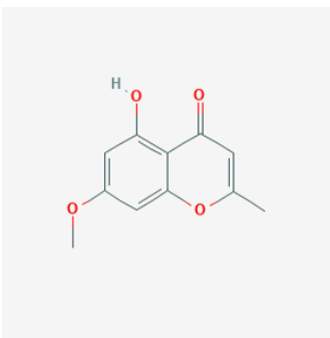
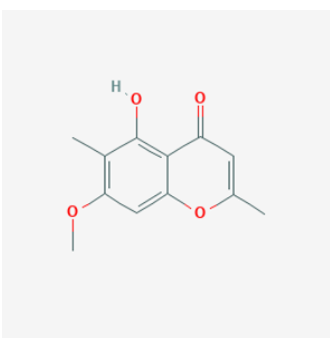
The COVID-19 3CLpro/Mpro (PDB ID: 6LU7) and free enzyme of the SARS-CoV-2 (2019- nCoV) main protease (PDB ID: 6Y2E) structures were obtained from the <https://www.rcsb.org/> website in PDB format. 3D structures of selected ligands (Table 1), obtained from the <https://pubchem.ncbi.nlm.nih.gov/> website in SDF format, were optimized by UCSF Chimera 1.14 software from <https://www.cgl.ucsf.edu/chimera/> and saved in MOL2 format.

2.2. Molecular docking

The COVID-19 3CLpro/Mpro (PDB ID: 6LU7) and main protease (PDB ID: 6Y2E) were prepared using autodock tools from the MGL Tools package <http://mgltools.scripps.edu/>. Water molecules and het atoms were removed, and polar hydrogen was added. Native positions of ligands on binding sites were determined by use of Autogrid with default settings ($x = -26,283$, $y = 12,599$, $z = 58,965$ at 1 Angstrom spacing). Ligand tethering to proteins was performed by genetic algorithm (GA) parameters, with 100 runs of GA criteria. The open source AutoDock Vina v.1.2.0. program (<https://vina.scripps.edu/>) was used to stimulate bioactive conformation, and the results were analyzed by Biovia Discovery Studio® Client 2020 (Dassault Systèmes BIOVIA, Discovery Studio Modeling Environment, Release 2017, San Diego: Dassault Systèmes, 2016).

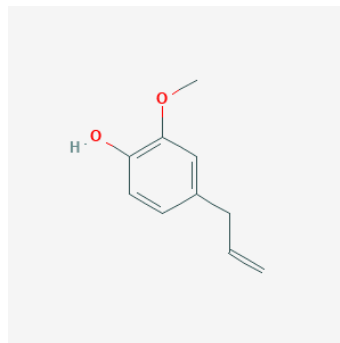
Table 1: Pubchem ID and structures of bioactive molecules from *Syzygium aromaticum*, *Citrus limon*, and *Allium sativum*.

| Plants | Compounds | CID | Structure | Formula |
|----------------------------|-------------|--------|--|--|
| <i>Syzygium aromaticum</i> | Biflorin | 441459 |  | C ₁₆ H ₁₈ O ₉ |
| | Campesterol | 173183 |  | C ₂₈ H ₄₈ O |

| | | | |
|-----------------|---------|--|-------------------|
| Carvacrol | 10364 |  | $C_{10}H_{14}O$ |
| Crategolic acid | 73659 |  | $C_{30}H_{48}O_4$ |
| Ellagic Acid | 5281855 |  | $C_{14}H_6O_8$ |
| Eugenin | 10189 |  | $C_{11}H_{10}O_4$ |
| Eugenitin | 3083581 |  | $C_{12}H_{12}O_4$ |

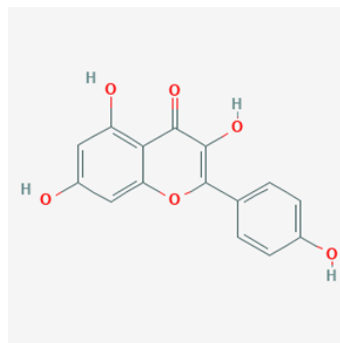
Eugenol

3314

 $C_{10}H_{12}O_2$

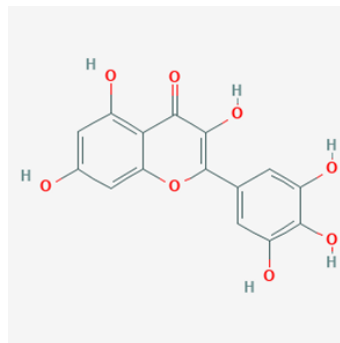
Kaempferol

5280863

 $C_{15}H_{10}O_6$

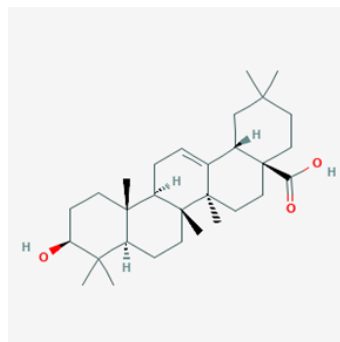
Myricetin

5281672

 $C_{15}H_{10}O_8$

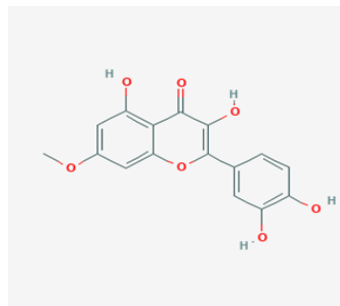
Oleanolic Acid

10494

 $C_{30}H_{48}O_3$

Rhamnetin

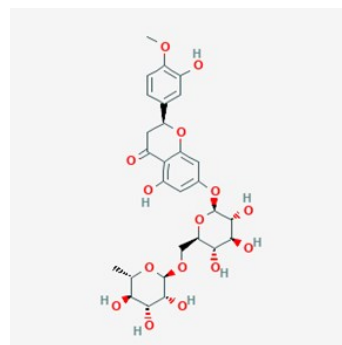
5281691

 $C_{16}H_{12}O_7$

Citrus limon

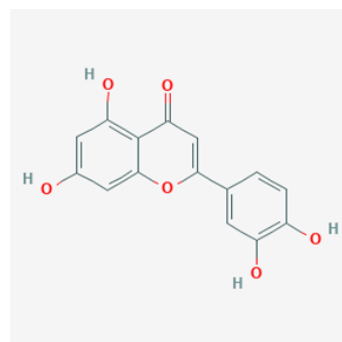
Hesperidin

10621

 $C_{28}H_{34}O_{15}$

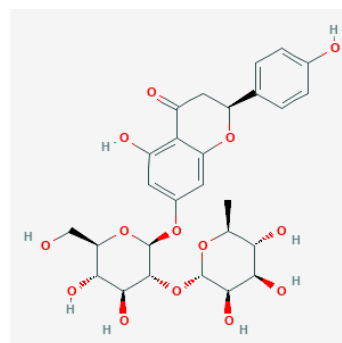
Luteolin

5280445

 $C_{15}H_{10}O_6$

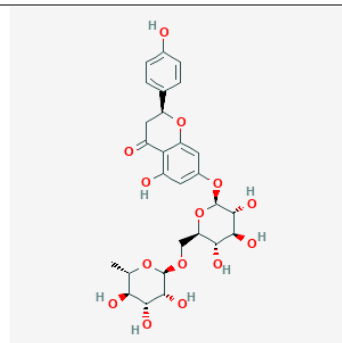
Naringin

442428

 $C_{27}H_{32}O_{14}$

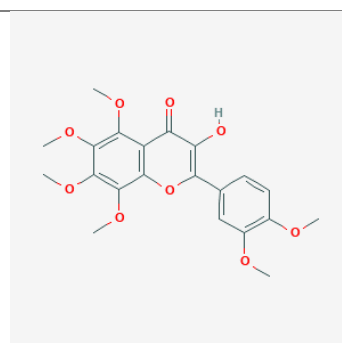
Narirutin

442431

 $C_{27}H_{32}O_{14}$

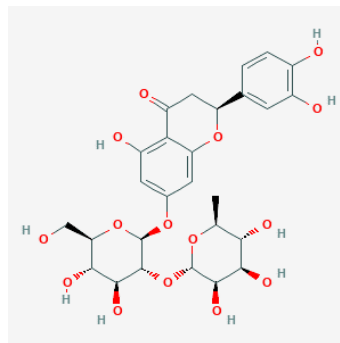
Natsudaaidain

3084605

 $C_{21}H_{22}O_9$

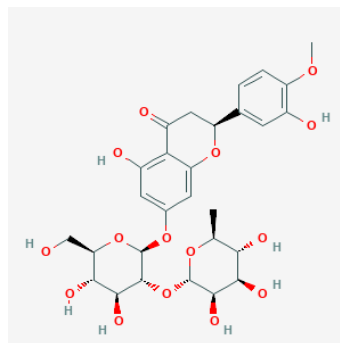
Neeriocitrin

114627

 $C_{27}H_{32}O_{15}$

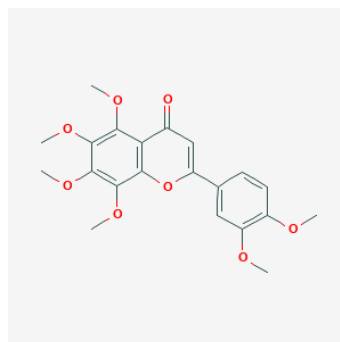
Neohesperidin

442439

 $C_{28}H_{34}O_{15}$

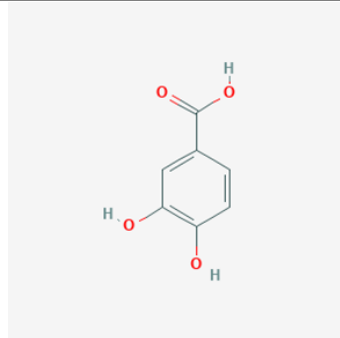
Nobiletin

72344

 $C_{21}H_{22}O_8$

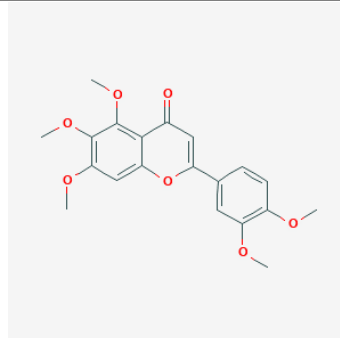
Protocatechuic acid

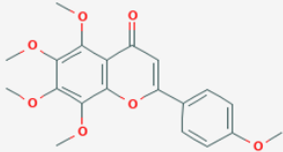
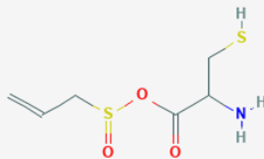
72


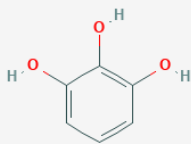
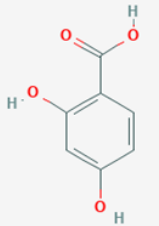
 $C_7H_6O_4$

Sinensetin

145659

 $C_{20}H_{20}O_7$

| | | | | |
|-----------------------|----------------------------|-----------|--|----------------------|
| | | |  | $C_{20}H_{20}O_7$ |
| | Tangeretin | 68077 | | |
| | | |  | $C_{27}H_{30}O_{15}$ |
| | Vicenin-2 | 442664 | | |
| | | |  | $C_6H_{10}OS_2$ |
| | Allicin | 65036 | | |
| <i>Allium sativum</i> | S-allyl-cysteine sulfoxide | 129668924 |  | $C_6H_{11}NO_3S_2$ |
| | Diallyl disulfide | 16590 |  | $C_6H_{10}S_2$ |

| | | | |
|----------------------|-------|--|--|
| Diallyl sulfide | 11617 |  | C ₆ H ₁₀ S |
| Pyrogallol | 1057 |  | C ₆ H ₆ O ₃ |
| Beta-Resorcylic acid | 1491 |  | C ₇ H ₆ O ₄ |

2.3. ADMET prediction

The absorption, metabolism, distribution, and excretion parameters were determined using the Qikprop function in the Maestro 11.5 version of the Schrödinger Software. The prediction was based on the physicochemical and pharmacokinetic properties of some molecules studied in our work, including molecular weight, a hydrogen bond acceptor and donor, total solvent surface area, the blood-brain partition coefficient, the octanol/water partition coefficient, and aqueous solubility (Chebbac et al., 2023).

2.4. Molecular Dynamic simulations

Modulating reactive molecular dynamics (MD) was performed using LAMMPS (Large scale Atomic/Molecular Massively Parallel Simulator) software and the ReaxFF force field. In this force field, the general energy function was described by the following Equation 1.

$$E_{\text{system}} = E_{\text{bond}} + E_{\text{over}} + E_{\text{under}} + E_{\text{val}} + E_{\text{pen}} + E_{\text{tors}} + E_{\text{conj}} + E_{\text{vdWaals}} + E_{\text{Coulomb}}$$

Where:

“*E_{bond}*” represents bond energy;

“*E_{over}*” and “*E_{under}*” denote over-and under-coordinated atoms in the energy contribution, respectively;

“*E_{val}*”, “*E_{pen}*”, “*E_{tors}*” are valence angle term, penalty energy, and torsion energy, respectively;

“*E_{conj}*”, “*E_{vdWaals}*”, “*E_{Coulomb}*” represent the conjugation effects to molecular energy, non-bonded van der Waals interaction, and Coulomb interaction, respectively.

At each step of MD simulations, this force field updates the bond orders and provides a pathway for bonds to form and break during the simulation of energy minimization. ReaxFF can reproduce with acuity all relevant quantum mechanical data, as well as provide atomistic descriptions of several complex chemical reactions. Simulations were done using target ligands, most similar to the structure of the protein, maintained at a constant temperature of 298 K. In MD simulations, the temperature was set based on displacement velocities of each atom/molecule. ReaxFF forcefield was applied with a timestep of 0.1 fs, so every interaction and

bond could be observed during the simulation. Reactions involving protein + ligand systems usually require a long time. The total number of interactions used in these simulations was 25 M, thus representing a timeframe of 2.5 ns. Although it might seem small, common methods of MD applied in these systems, such as CHARMM forcefield, use time steps of 2 fs, which is 8 times longer than the one used in ReaxFF, so the timeframe of both methods can be equated. The calculation time of each simulation was approximately 700 hrs. ReaxFF is not commonly used in these systems because it was initially built for analyzing fast reactions or complex mechanisms. However, using bond orders to determine association energies can help analyze interactions between large structures and ligands. Physical interactions or chemical bonds can be observed, and thus behaviors of ligands and overall binding energy/stabilization of systems can be predicted.

Four cases of systems of protein + ligand were chosen for the simulations:

Case 1: 6LU7 + Hesperidin;

Case 2: 6Y2E + Hesperidin;

Case 3: 6LU7 + Diosmin;

Case 4: 6Y2E + Diosmin.

The system was minimized using low-temperature (5K) molecular dynamics. After minimization, for the equilibration phase, the NVT ensemble (canonical, with a constant number of atoms, volume, and temperature) was used, and for the production phase, the NVE ensemble was employed with a constant number of atoms (N), constant volume (V) and control of the potential energy (E). Temperatures were controlled by the Berendsen thermostat, with a temperature damping constant of 50 fs (Figure 1).

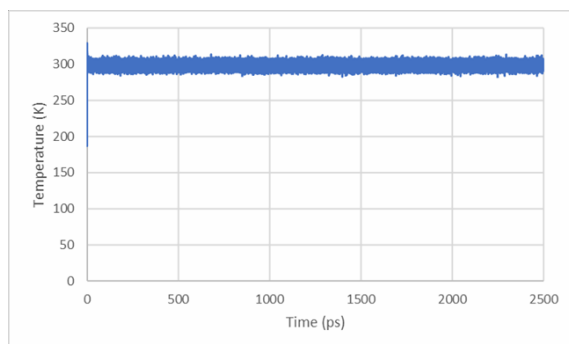


Figure 1: Temperature variation during simulations.

3. Results and discussion

3.1. Molecular Docking

In total, 34 natural products belonging to the three medicinal plants were docked to estimate binding affinities between each natural compound and the two proteases, 6LU7 and 6Y2E (Table 2). Compared to chloroquine, a controller drug with binding energy equal to -6 kcal/mol, which was selected as the reference molecule (Edache et al., 2022), for protease 6LU7, 24 compounds exhibited binding affinities greater

than or equal to -6 Kcal/mol. Ellagic acid, narirutin, neoeriocitrin, and neohesperidin exhibited interaction energies equal to -8.4 kcal/mol. Diosmin had binding energy of -7.8 kcal/mol, while kaempferol and hesperidin had energies of -7.6 kcal/mol, crategolic acid and oleanolic acid had a value of -7.5 kcal/mol, and luteolin and naringin had binding energies of -7.4 kcal/mol. Six natural products studied exhibited binding affinities for 6Y2E protease greater than or equal to -6 Kcal/mol. In addition to oleanolic acid, diosmin, eriocitrin hesperidin, and neohesperidin, which are active on the 6LU7 site, are also active on the 6Y2E site with different energy between the two proteases (Table 2). Ellagic acid is a polyphenol in various medicinal plants and vegetables, such as *Syzygium aromaticum* (Batiha et al., 2020) that exhibits antioxidant, anticarcinogenic, and chemopreventive activities (Ismail et al., 2016; Moktar et al., 2009; Narayanan et al., 1999). Ellagic acid, on top of its various therapeutic potentials, including in vitro anticancer activity (Narayanan et al., 1999), has an IC₅₀ for antiviral activity of 1.4 μ M and 6.4 μ M against Ebola virus (EBOV) and Marburg virus (MARV) pseudovirions, respectively (Cui et al., 2018). In addition, its activities against Zika and human rhinoviruses (HRV) have been demonstrated (Acquadro et al., 2020; Park et al., 2014). Narirutin, neoeriocitrin, neohesperidin, diosmin, and hesperidin, the predominant flavanone-7-O-glycosides present in citrus fruits, are known to have antioxidant, anticancer, antiviral, and anti-inflammatory activities (Aturki et al., 2004). Based on virtual screening with computational simulations, narirutin and hesperidin had a significantly higher docking score than indicated that they would be more effective against H1N1 infection than the currently marketed anti-influenza drug Oseltamivir (Tamiflu) (Sharma et al., 2011). Hesperidin, neohesperidin, and diosmin have also been effective against human rotavirus (Ben-Shabat et al., 2020).

Kaempferol, a natural flavonoid, exhibits antioxidant, anti-inflammatory, antimicrobial, antidiabetic, anticancer, and antiviral activities. Antiviral activity of kaempferol has been reported against human cytomegalovirus (Mitrocotsa et al., 2000), human immunodeficiency virus 1 (HIV-1) (Behbahani et al., 2014), Japanese encephalitis virus (JEV) (Care et al., 2020) and coronaviruses (Schwarz et al., 2014). In the current study, molecular docking predicted that binding occurs between kaempferol and SARS-CoV-2 6LU7 and 6Y2E proteases with high affinities of -7.6 and 5.2 kcal/mol, respectively (Table 2). Our findings are corroborated by a previous computational simulation study indicating that the observed high affinity of kaempferol for the substrate binding pocket of the main SARS-CoV-2 protease (3CLPro) proceeds through both hydrophobic interactions and hydrogen bonding with the active site residues, such as His41 and Cys145 (Rehman et al., 2021). Therefore, this observation strongly advocates using natural flavonoids as potent SARS-CoV-2 control agents.

Oleanolic acid is a biologically active pentacyclic triterpenoid in more than 1620 plants (Pollier and Goossens, 2012). Oleanolic acid has been reported to exhibit antioxidant (Ovesná et al., 2006; Somova et al., 2003; Sultana and Ata, 2008), anticancer (Dzubak et al., 2006), anti-inflammatory (Petronelli et al., 2009), antibacterial (Hichri et al., 2003) and antiviral activities (Kong et al., 2013). Oleanolic acid has been confirmed to have broad antiviral activities against HIV (Zhu et al., 2001), influenza (Yu et al., 2006), HCV (Kong et al., 2013), and HSV-1 (Ikeda et al., 2005) viruses.

Biflorin, another compound extracted from *Syzygium aromaticum*, is a natural O- naphthoquinone known for its solid anticancer activity (de Vasconcellos et al., 2007; Montenegro et al., 2013). The antiviral activities of biflorin have been recently reported against DENV, taking place through the inhibition of its proteases (Saleem et al., 2019).

For interactions between the different bioactive molecules and proteases 6LU7 and 6Y2E, hydrogen bonds in the complex explain the strength of association between natural products and proteases (Table 3). Hydrogen bonds are considered first-level interactions, while other types of interactions, such as interactions between p systems and cation -p interactions and hydrophobic contacts while non-specific, Van der Waals interactions are considered second and third-level interactions, respectively (Aanouz et al.,

2021). Natural product molecules with maximum binding affinities equal to -8.4 kcal/mol exhibited good hydrogen bonds with 6LU7 and 6Y2E protease. For example, diosmin has 3 hydrogen bonds with 6LU7 protease: ILE249, GLN110, and GLN107, while it is 4 hydrogen bonds with 6Y2E protease: ALA7, GLU14, SER10, GLY11, THR304, PHE305, ARG298 (Table 3 and Figure 2). Despite the known antiviral activity of garlic, their organosulfur compounds, such as allicin, S-allyl-cysteine sulfoxide, diallyl disulfide, diallyl sulfide, diallyl trisulfide, and S-allyl-cysteine present a weak band affinity which does not exceed -4.3 kcal/mol for 6LU7 and 6Y2E protease (Table 2).

3.2. ADME analysis

Additionally, predicted ADME showed acceptable human oral absorption for ellagic acid, kaempferol and biflorin of 43.6%, 67.5% and 44.8% respectively. Whereas the permeability in the intestinal barriers expressed bay Caco-2 of these three molecules is 33.429, 163.1, and 187.9 nm/s respectively.

Blood-brain partition coefficients were indicated on the capacity of the molecule to cross the blood-brain barrier. Biflorin presented an accepted value between -3 and 1.2. Whereas Ellagic acid and kaempferol showed unacceptable values higher than 1.2 (Table 4).

Table 2: Binding affinities between natural compounds and proteases 6LU7 or 6Y2E.

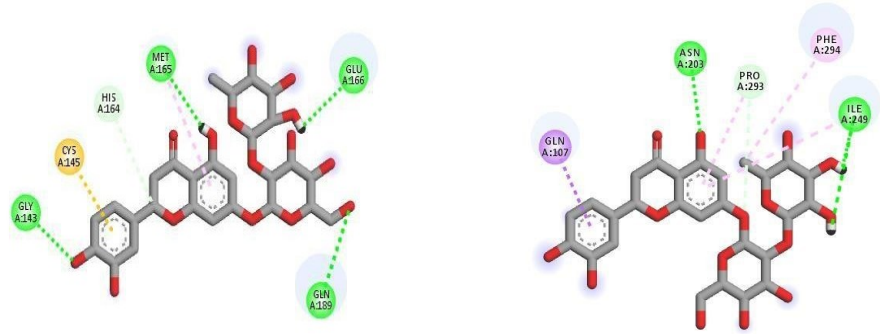
| Compound name | Binding affinity (Kcal/mol) 6LU7 protease | Binding affinity (Kcal/mol) 6Y2E protease |
|---------------------|--|--|
| Biflorin | -6.7 | -6.9 |
| Campesterol | -6.8 | -5.0 |
| Carvacrol | -5.2 | -4.4 |
| Crategolic acid | -7.5 | -5.3 |
| Ellagic Acid | -8.4 | -5.7 |
| Eugenin | -6.0 | -4.9 |
| Eugenitin | -6.0 | -5.0 |
| Eugenol | -5.5 | -5.0 |
| Kaempferol | -7.6 | -5.1 |
| Myricetin | -6.7 | -5.1 |
| Oleanolic Acid | -7.5 | -7.1 |
| Rhamnetin | -7.3 | -5.2 |
| Stigmasterol | -7.0 | -5.0 |
| Vanillin | -5.0 | -3.4 |
| Diosmin | -7.8 | -7.7 |
| Eriocitrin | -8.0 | -6.0 |
| Hesperidin | -7.6 | -8.1 |
| Luteolin | -7.4 | -5.4 |
| Naringin | -7.4 | -5.4 |
| Narirutin | -8.4 | -5.8 |
| Natsudaaidain | -6.5 | -5.0 |
| Neoeriocitrin | -8.4 | -5.5 |
| Neohesperidin | -8.4 | -6.2 |
| Nobiletin | -6.4 | -5.2 |
| Protocatechuic acid | -5.4 | -5.0 |

| | | |
|----------------------------|------|------|
| Sinensetin | -6.3 | -5.2 |
| Tangeretin | -6.1 | -5.0 |
| Vicenin-2 | -7.5 | -2.5 |
| Allicin | -3.7 | -2.8 |
| S-allyl-cysteine sulfoxide | -4.3 | -4.0 |
| diallyl disulfide | -2.9 | -2.5 |
| diallyl sulfide | -3.0 | -2.5 |
| Pyrogallol | -4.9 | -3.5 |
| β-Resorcylic acid | -5.7 | -5.3 |

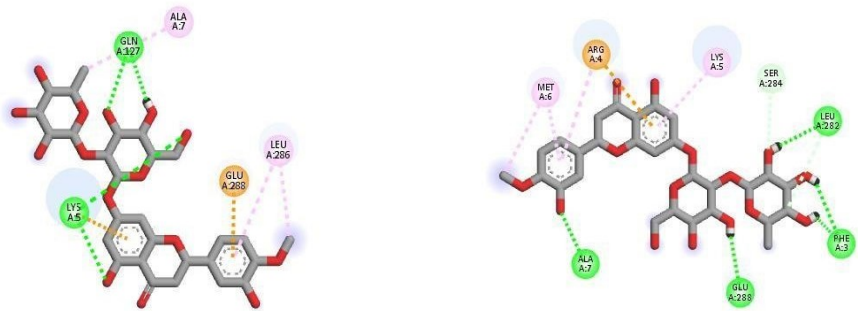
Table 3: Most potent interactions between the different bioactive molecules and proteases 6LU7 and 6Y2E.

| Compound | Binding conformation of compounds at the active site of Coronavirus (2019-nCoV) | |
|------------|---|---------------|
| | 6LU7 protease | 6Y2E protease |
| Diosmin | | |
| Hesperidin | | |
| Narirutin | | |

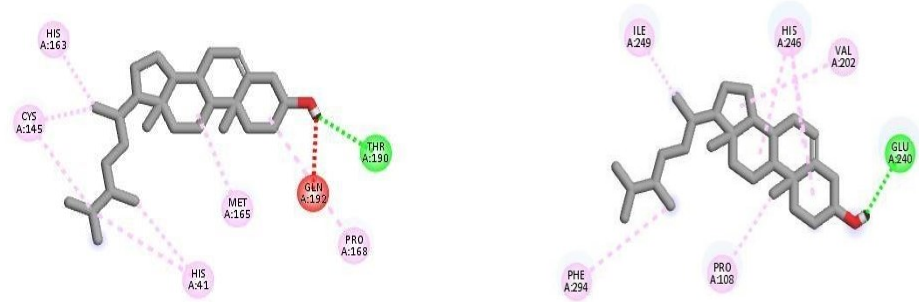
Neeriocitrin



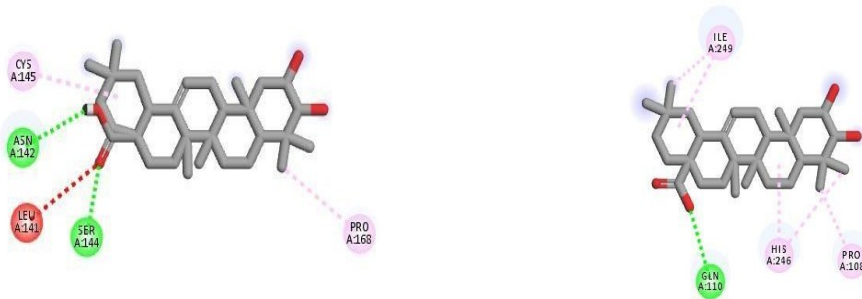
Neohesperidin



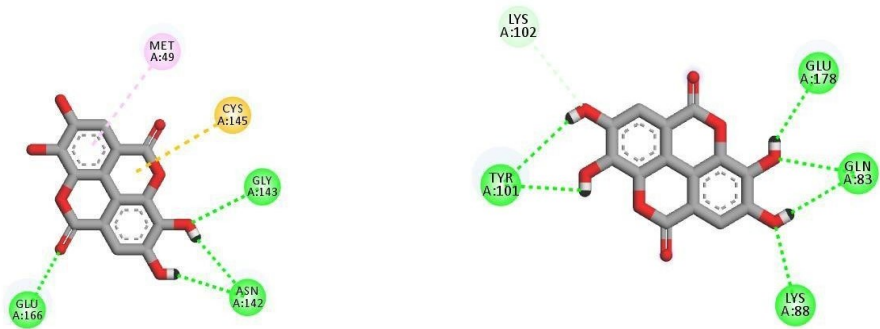
Campesterol



Crategolic acid



Ellagic acid



Kaempferol

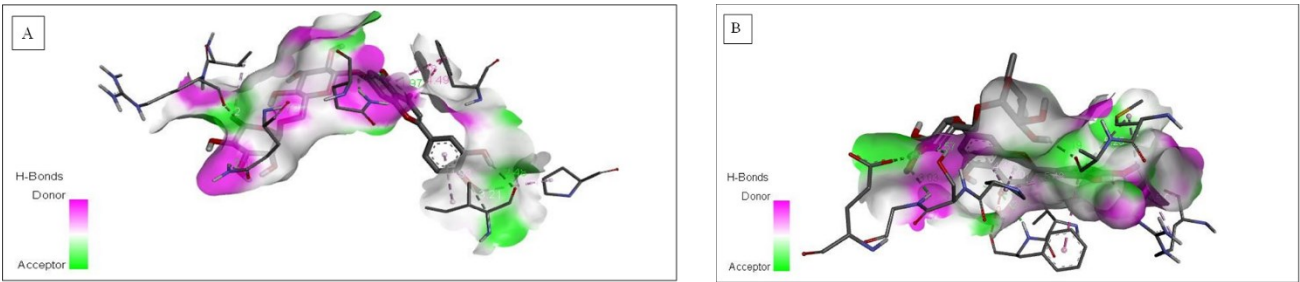
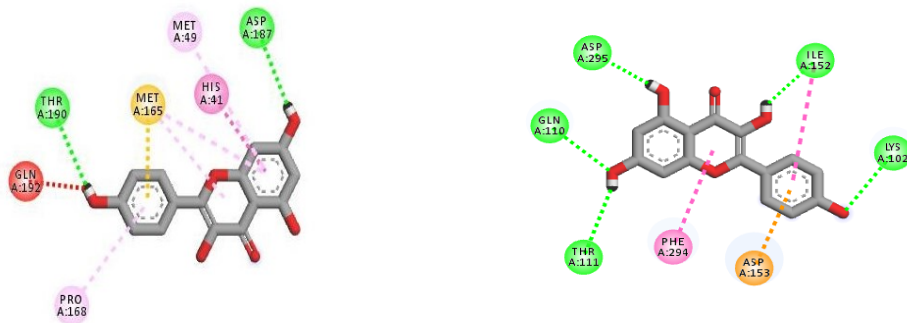


Figure 2: 3D Binding conformations of the diosmin inhibitor at 6LU7 protease (A) or 6Y2E protease (B) spike protein (Hydrogen Bond interaction).

Table 4: ADME properties some molecules as COVID-19 inhibitors

| Compound Name | MM ^a | Donors HB ^b | Acceptors HB ^c | SASA ^d | QPP Caco ^e | QP logPo/w ^f | QPlog BB ^g | QP logS ^h | % Human Oral Absorption ⁱ |
|---------------|-----------------|------------------------|---------------------------|-------------------|-----------------------|-------------------------|-----------------------|----------------------|--------------------------------------|
| Ellagic acid | 302.197 | 0 | 6 | 349.905 | 33.429 | -1.811 | -1.673 | 0.945 | 43.621 |
| Kaempferol | 286.24 | 1 | 4 | 427.511 | 136.169 | 0.41 | -1.502 | -2.107 | 67.543 |
| Biflorin | 354.313 | 5.5 | 10.25 | 453.254 | 187.931 | -1.684 | -1.161 | -2.532 | 44.826 |

^a mass of molecules (acceptable range: 500 mol). ^b Donor of hydrogen bonds (acceptable range: ≤5). ^c Acceptor of hydrogen bonds (acceptable range: ≤10). ^d Total solvent accessible surface area using a probe with a 1.4 radius (acceptable range: 300–1000 radius). ^e QPP Caco: Predicted apparent Caco-2 cell permeability in nm/s. Caco-2 cells is a model for the gut-blood barrier (<25-poor, >500-great). ^f Predicted octanol/water partition coefficient (acceptable range: -2 –6.5). ^g Predicted blood–brain partition coefficient (acceptable range: -3 –1.2). ^h Predicted aqueous solubility, S in mol/dm⁻³ (acceptable range: -6.5–0.5). ⁱ Predicted human oral absorption on 0 to 100% scale (<25% is poor and >80% is high).

3.3. MD simulations

The simulations aimed to observe whether the ligand would bind to the protein, and which would be the energy variation

of this process. Therefore, the behavior could be analyzed. Unit cells of the systems were built with the protein plus the ligand, with a minimum distance from each other of 20 Å, so

after minimization, both would be kept in approximately the same place. Simulations using the ReaxFF force field require small timesteps, so every bond break or formation is accurately observed. In all four cases, the ligand succeeded in binding with the protein during the production phase. The system's total energy decreased significantly, showing greater stabilization of the system with both structures bonded together. During optimization structure of ligands experienced rotation, possibly due to the protein branches. Dipole/electrostatic interactions are constantly evaluated during the simulations, so the ligand (smaller structure) is expected to adapt to the protein surface for the most favorable bonding. For instance, the hesperidin binding to 6LU7, from the beginning of the simulation to the complete binding of the ligand, occurred at 80 ps after the beginning but was finished at approximately 120 ps from the start (Figure 3). Hesperidin rotates before reaching the protein surface, and the approach becomes faster when the intermolecular interactions become stronger. The variation observed in the system's total energy was approximately $\Delta E = -11695.5$ kJ/mol (Figure 4). The greatest energy variation occurs in the first 25 ps. Since the system was minimized at 5K and then kept at 200 K during the equilibration phase, there is a rearrangement of the structures when applying 298 K in the production phase, thus stabilizing the system with this new parameter. This behavior is expected and observed in all 4 cases simulated.

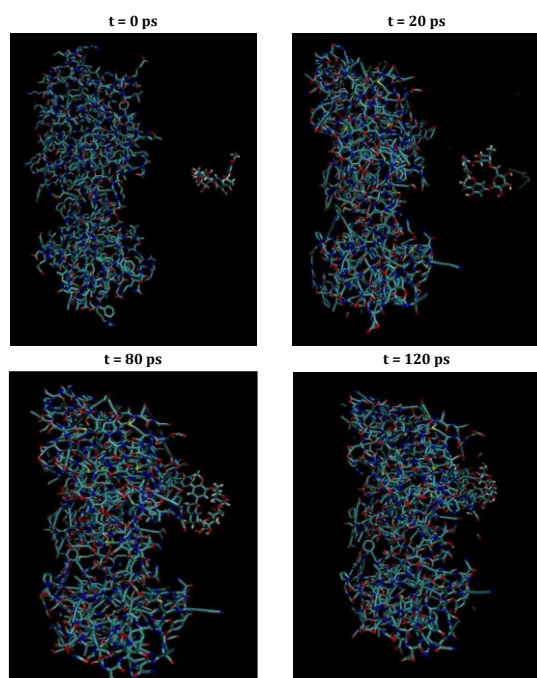


Figure 3: Time-lapse of case 1, from the start to the complete binding of the ligand to the protein.

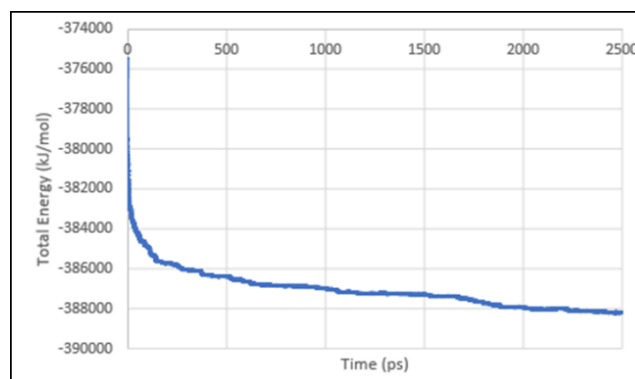


Figure 4: Total energy variation during the production phase of the RMD simulation for case 1.

The interaction of hesperidin with 6Y2E (case 2) was slower than the interaction with 6LU7 (case 1). After 120 ps from the beginning of the production phase, the ligand was still approaching the protein structure. Binding started at approximately 200 ps after the start, then took approximately 300 ps to complete. Thus, based on the difference in velocities, it seems that hesperidin has more affinity to 6LU7 than to 6Y2E. However, this simulation's total energy variation (Figure 5) was $\Delta E = -20495.7$ kJ/mol, almost double that observed in case 1. Therefore, even though kinetics were slower, the interaction between hesperidin and 6Y2E was more substantial than with 6LU7, which might result in a better performance of the ligand in deactivating the active site of the protein (Figure 6).

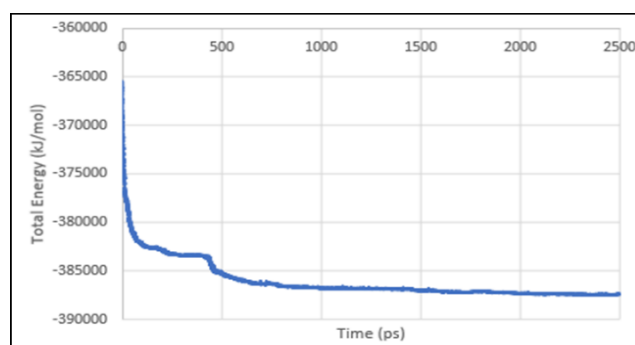


Figure 5: Total energy variation during the production phase of the RMD simulation for case 2.

The binding of diosmin to 6LU7 or 6Y2E was evaluated in cases 3 and 4, respectively. In case 3, the ligand took almost 100 ps to approach and interact with the protein structure. After the initial interaction, the ligand was utterly bound to the protein surface only after 400 ps from the beginning of the production phase (Figure 7). Since the energy evaluation shows a difference of $\Delta E = -12787.5$ kJ/mol from the beginning, the system becomes more stable, indicating a solid binding between protein and ligand (Figure 8). In comparison to case 1, 6LU7 shows a stronger binding with Hesperidin than with diosmin, but as the difference is small (~10%), perhaps the kinetics presents a more important

figure in this scenario. The complete bond of the ligand in case 3 is 3 times slower than in case 1, so possibly Hesperidin could be a more suitable ligand for protein 6LU7.

The last system evaluated was the binding of diosmin with 6Y2E (case 4). Among all systems, this was the one with the fastest kinetics. Thereby, the approach of the ligand to the protein surface was the fastest. After 35 ps from the beginning of the production phase, the ligand was remarkably close to the protein 6Y2E, showing a probable high interaction (dipole, Van der Waals, etc.) between the ligand and 6Y2E (Figure 9). Some rearrangements (rotation) of diosmin were observed, but after 200 ps, the ligand was completely bound to the protein. When comparing this system with case 2 (6Y2E + hesperidin), it is observed that the overall kinetics and energy (Figure 10) of case 4 favor diosmin as a more suitable ligand for protein 6Y2E, with a total energy variation of $\Delta E = -21695$ kJ/mol. Therefore, faster coupling and the greatest variation in energy make this ligand the most favorable option for this protein and, thus, a likely therapeutic agent to treat COVID-19.

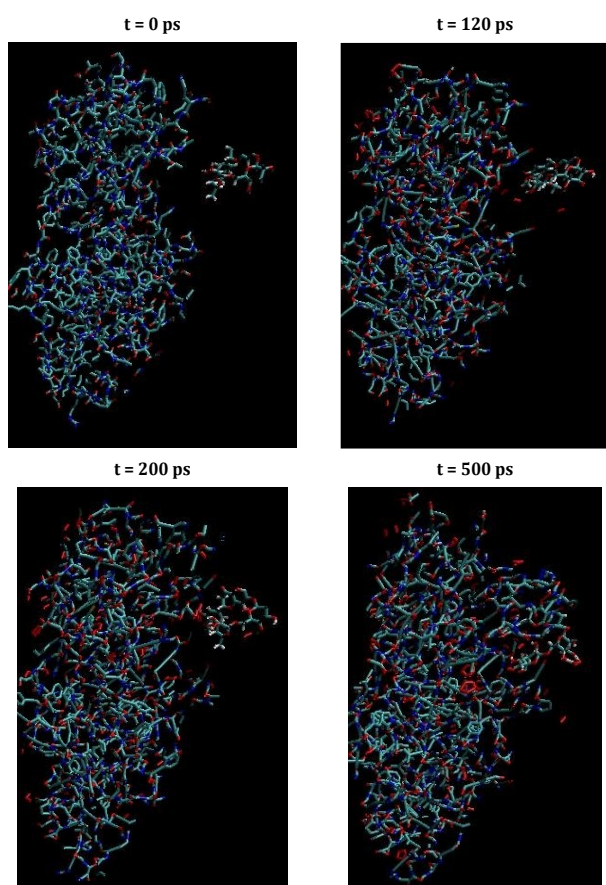


Figure 6: Time-lapse of case 2, from the start to the complete binding of the ligand to the protein

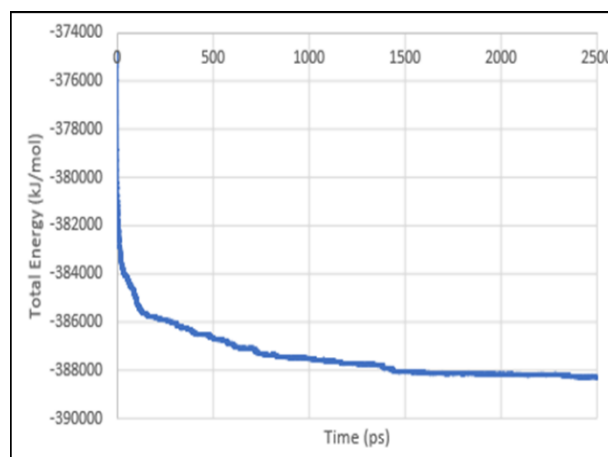


Figure 7: Total energy variation during the production phase of the RMD simulation for case 3.

The last system evaluated was the binding of diosmin with 6Y2E (case 4). Among all systems, this was the one with the fastest kinetics. Thereby, the approach of the ligand to the protein surface was the fastest. After 35 ps from the beginning of the production phase, the ligand was remarkably close to the protein 6Y2E, showing a probable high interaction (dipole, Van der Waals, etc.) between the ligand and 6Y2E (Figure 9). Some rearrangements (rotation) of diosmin were observed, but after 200 ps, the ligand was completely bound to the protein. When comparing this system with case 2 (6Y2E + hesperidin), it is observed that the overall kinetics and energy (Figure 10) of case 4 favor diosmin as a more suitable ligand for protein 6Y2E, with a total energy variation of $\Delta E = -21695$ kJ/mol. Therefore, a faster coupling and the greatest variation in energy make this ligand the most favorable option for this protein and, thus, a likely therapeutic agent to treat COVID-19.

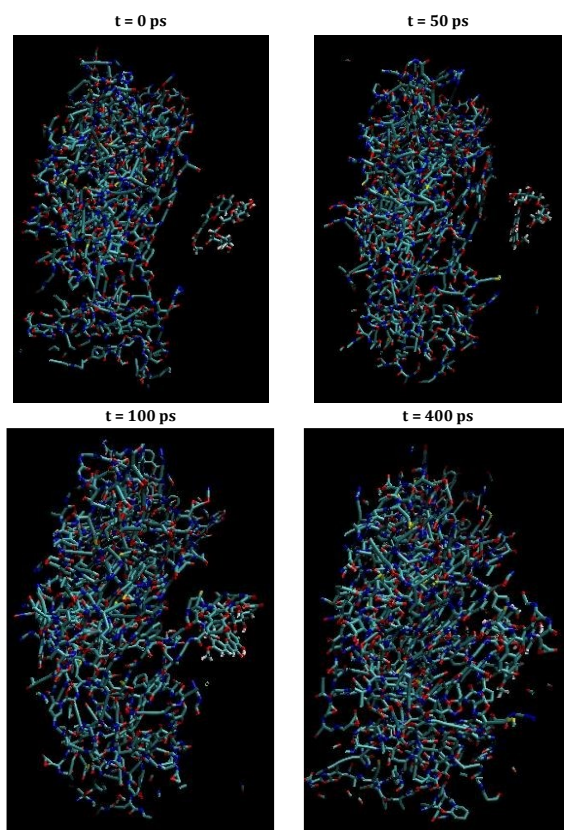


Figure 8: Time-lapse of case 3, from the start to the complete binding of the ligand to the protein.

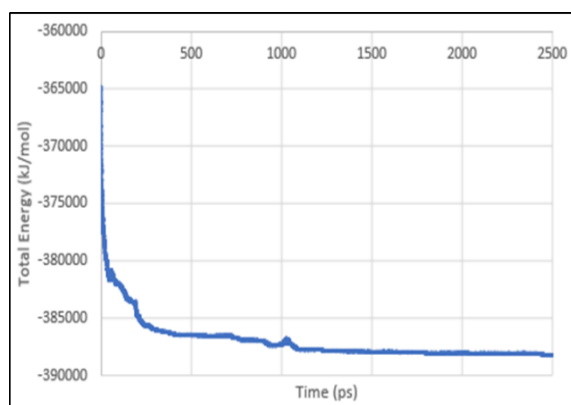


Figure 9: Total energy variation during the production phase of the RMD simulation for case 4.

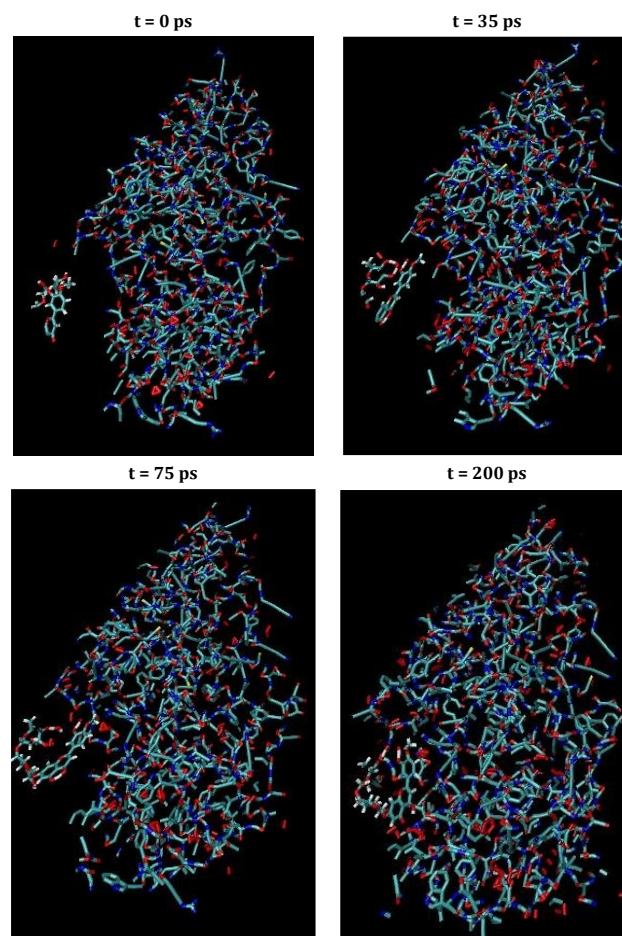


Figure 10: Time-lapse of case 4, from the start to the complete binding of the ligand to the protein.

4. Conclusion

Based on binding to the critical proteases of SARS-CoV-2, 6LU7, and 6Y2E, as determined by computational virtual screening, ellagic acid, narirutin, neoeriocitrin and neohesperidin isolated from medicinal plants under investigation exhibited potential as inhibitors of SARS-CoV-2. Clinical trials assessing the anti-SARS-CoV-2 activities of these compounds on COVID-19 patients seem appropriate and highly warranted to further verify their molecular targets and therapeutic potential. Additionally, evaluating the effective concentrations and toxicity of these molecules is essential. Experimental validation of the inhibitory activity of these compounds against the target enzymes to confirm their affinities is highly recommended.

Acknowledgment

Prof. Giesy was supported by the Canada Research Chairs Program of the Natural Sciences and Engineering Research Council of Canada (NSERC) and a Distinguished Visiting Professorship from the Department of Environmental Sciences, at Baylor University in Waco, Texas, USA.

Funding

This research received no external funding

Conflicts of Interest

The authors declare no conflicts of interest.

Data availability statement

Data will be available upon request from the corresponding author.

References

- Aanouz, I., Belhassan, A., El-Khatibi, K., Lakhli, T., El-Ldrissi, M., Bouachrine, M., 2021. Moroccan Medicinal plants as inhibitors against SARS-CoV-2 main protease: Computational investigations. *Journal of Biomolecular Structure and Dynamics* 39(8), 2971-2979. <https://doi.org/10.1080/07391102.2020.1758790>
- Aboubakr, H.A., Nauertz, A., Luong, N.T., Agrawal, S., El-Sohaimy, S.A., Youssef, M.M., Goyal, S.M., 2016. In vitro antiviral activity of clove and ginger aqueous extracts against feline calicivirus, a surrogate for human norovirus. *Journal of food protection* 79(6), 1001-1012. <https://doi.org/10.4315/0362-028X.JFP-15-593>
- Acquadro, S., Civra, A., Cagliero, C., Marengo, A., Rittà, M., Francese, R., Sanna, C., Berte, C., Sgorbini, B., Lembo, D., 2020. Punica granatum leaf ethanolic extract and ellagic acid as inhibitors of Zika virus infection. *Planta medica* 86(18), 1363-1374. <https://doi.org/10.1055/a-1232-5705>
- Aturki, Z., Brandi, V., Sinibaldi, M., 2004. Separation of flavanone-7-O-glycoside diastereomers and analysis in citrus juices by multidimensional liquid chromatography coupled with mass spectrometry. *Journal of agricultural and food chemistry* 52(17), 5303-5308. <https://doi.org/10.1021/jf0400967>
- Batiha, G.E.-S., Alkazmi, L.M., Wasef, L.G., Beshbishy, A.M., Nadwa, E.H., Rashwan, E.K., 2020. Syzygium aromaticum L.(Myrtaceae): Traditional uses, bioactive chemical constituents, pharmacological and toxicological activities. *Biomolecules* 10(2). <https://doi.org/10.3390/biom10030352>
- Behbahani, M., Sayedipour, S., Pourazar, A., Shansazzadeh, M., 2014. In vitro anti-HIV-1 activities of kaempferol and kaempferol-7-O-glucoside isolated from Securigera securidaca. *Research in pharmaceutical sciences* 9(6), 463-469.
- Ben-Shabat, S., Yarmolinsky, L., Porat, D., Dahan, A., 2020. Antiviral effect of phytochemicals from medicinal plants: Applications and drug delivery strategies. *Drug delivery and translational research* 10, 354-367. <https://doi.org/10.1007/s13346-019-00691-6>
- Bourhia, M., Amrati, F.E.-Z., Ullah, R., Alqahtani, A.S., Boust, D., Ibenmoussa, S., Khlil, N., 2020. Coronavirus treatments: what drugs might work against COVID-19? *Natural Product Communications* 15(7), 1934578X20945442. <https://doi.org/10.1177/1934578X20945442>
- Care, C., Sornjai, W., Jaratsittisin, J., Hitakarun, A., Wikan, N., Triwitayakorn, K., Smith, D.R., 2020. Discordant activity of kaempferol towards dengue virus and Japanese encephalitis virus. *Molecules* 25(5), 1246. <https://doi.org/10.3390/molecules25051246>
- Chaachouay, N., Douira, A., Zidane, L., 2021. COVID-19, prevention and treatment with herbal medicine in the herbal markets of Salé Prefecture, North-Western Morocco. *European journal of integrative medicine* 42, 101285. <https://doi.org/10.1016/j.eujim.2021.101285>
- Chebaibi, M., Boust, D., Bourhia, M., Baammi, S., Salamatullah, A.M., Nafidi, H.-A., Hoummami, H., Achour, S., 2022. Ethnobotanical Study of Medicinal Plants Used against COVID-19. *Evidence-Based Complementary and Alternative Medicine* 2022(1), 2085297. <https://doi.org/10.1155/2022/2085297>
- Chebbac, K., Benziane Ouaritini, Z., El Moussaoui, A., Chebaibi, M., Salamatullah, A.M., Lafraxo, S., Bourhia, M., Giesy, J.P., Aboul-Soud, M.A., Guemmouh, R., 2023. In vitro and in silico studies of antimicrobial, and antioxidant activities of chemically characterized essential oil of artemisia flahaultii L.(Asteraceae). *Life* 13(3), 779. <https://doi.org/10.3390/life13030779>
- Cortés-Rojas, D.F., de Souza, C.R.F., Oliveira, W.P., 2014. Clove (*Syzygium aromaticum*): a precious spice. *Asian Pacific journal of tropical biomedicine* 4(2), 90-96. [https://doi.org/10.1016/S2221-1691\(14\)60215-X](https://doi.org/10.1016/S2221-1691(14)60215-X)
- Costanzo, M., De Giglio, M.A., Roviello, G.N., 2020. SARS-CoV-2: recent reports on antiviral therapies based on lopinavir/ritonavir, darunavir/umifenovir, hydroxychloroquine, remdesivir, favipiravir and other drugs for the treatment of the new coronavirus. *Current medicinal chemistry* 27(27), 4536-4541. <https://doi.org/10.2174/0929867327666200416131117>
- Cui, Q., Du, R., Anantpadma, M., Schafer, A., Hou, L., Tian, J., Davey, R.A., Cheng, H., Rong, L., 2018. Identification of ellagic acid from plant *Rhodiola rosea* L. as an anti-Ebola virus entry inhibitor. *Viruses* 10(4), 152. <https://doi.org/10.3390/v10040152>
- de Vasconcellos, M.C., Bezerra, D.P., Fonseca, A.M., Pereira, M.R.P., Lemos, T.L.G., Pessoa, O.D.L., Pessoa, C., de Moraes, M.O., Alves, A.P.N.N., Costa-Lotuf, L.V., 2007. Antitumor activity of biflorin, an o-naphthoquinone isolated from *Capraria biflora*. *Biological and Pharmaceutical Bulletin* 30(8), 1416-1421. <https://doi.org/10.1248/bpb.30.1416>
- Del Río, J., Fuster, M., Gómez, P., Porras, I., García-Lidón, A., Ortuño, A., 2004. Citrus limon: A source of flavonoids of pharmaceutical interest. *Food chemistry* 84(3), 457-461. [https://doi.org/10.1016/S0308-8146\(03\)00272-3](https://doi.org/10.1016/S0308-8146(03)00272-3)
- Dzubak, P., Hajduch, M., Vydra, D., Hustova, A., Kvasnica, M., Biedermann, D., Markova, L., Urban, M., Sarek, J., 2006. Pharmacological activities of natural triterpenoids and their therapeutic implications. *Natural*

- product reports 23(3), 394-411. <https://doi.org/10.1039/B515312N>
- Edache, E., Uzairu, A., Mamza, P., Shallangwa, G., 2022. A 2D-QSAR, homology modeling, docking, ADMET, and molecular dynamics simulations studies for assessment of a novel SARS-Cov-2 and *Pseudomonas aeruginosa* inhibitors. *J Virol Viral Dis* 2(2). <https://doi.org/10.54289/JVVD2200106>
- Eriani, G., Martin, F., 2022. Viral and cellular translation during SARS-CoV-2 infection. *FEBS Open Bio* 12(9), 1584-1601. <https://doi.org/10.1002/2211-5463.13413>
- Fenwick, G., Hanley, A., 1985. Allium species poisoning. *The Veterinary Record* 116(1), 28-28. <https://doi.org/10.1136/vr.116.1.28>
- Hichri, F., Jannet, H.B., Cheriaa, J., Jegham, S., Mighri, Z., 2003. Antibacterial activities of a few prepared derivatives of oleanolic acid and of other natural triterpenic compounds. *Comptes rendus. Chimie* 6(4), 473-483. <https://doi.org/10.1136/vr.116.1.28>
- Ikeda, T., Yokomizo, K., Okawa, M., Tsuchihashi, R., Kinjo, J., Nohara, T., Uyeda, M., 2005. Anti-herpes virus type 1 activity of oleanane-type triterpenoids. *Biological and Pharmaceutical Bulletin* 28(9), 1779-1781. <https://doi.org/10.1248/bpb.28.1779>
- Ismail, T., Calcabrini, C., Diaz, A.R., Fimognari, C., Turrini, E., Catanzaro, E., Akhtar, S., Sestili, P., 2016. Ellagitannins in cancer chemoprevention and therapy. *Toxins* 8(5), 151. <https://doi.org/10.3390/toxins8050151>
- Kanyinda, J.-N.M., 2020. Coronavirus (COVID-19): a protocol for prevention and treatment (Covalyse®). *European Journal of Medical and Health Sciences* 2(3). <https://doi.org/10.24018/ejmed.2020.2.4.340>
- Khaerunnisa, S., Kurniawan, H., Awaluddin, R., Suhartati, S., Soetjipto, S., 2020. Potential inhibitor of COVID-19 main protease (Mpro) from several medicinal plant compounds by molecular docking study. *Preprints* 2020, 2020030226. <https://doi.org/10.20944/preprints202003.0226.v1>
- Kong, L., Li, S., Liao, Q., Zhang, Y., Sun, R., Zhu, X., Zhang, Q., Wang, J., Wu, X., Fang, X., 2013. Oleanolic acid and ursolic acid: novel hepatitis C virus antivirals that inhibit NS5B activity. *Antiviral research* 98(1), 44-53. <https://doi.org/10.1016/j.antiviral.2013.02.003>
- Mercatelli, D., Holding, A.N., Giorgi, F.M., 2021. Web tools to fight pandemics: the COVID-19 experience. *Briefings in bioinformatics* 22(2), 690-700. <https://doi.org/10.1093/bib/bbaa261>
- Mitrocotsa, D., Mitaku, S., Axarlis, S., Harvala, C., Malamas, M., 2000. Evaluation of the antiviral activity of kaempferol and its glycosides against human cytomegalovirus. *Planta medica* 66(04), 377-379. <https://doi.org/10.1055/s-2000-8550>
- Moktar, A., Ravoory, S., Vadhanam, M.V., Gairola, C.G., Gupta, R.C., 2009. Cigarette smoke-induced DNA damage and repair detected by the comet assay in HPV-transformed cervical cells. *International journal of oncology* 35(6), 1297-1304. <https://doi.org/10.3892/ijo.00000447>
- Montenegro, R., Burbano, R., Silva, M., Lemos, T., Vasconcellos, M., 2013. Biflorin, a naphthoquinone, inhibitsegfr in breast cancer cells. *Med chem* 3, 179-182. <https://doi.org/10.4172/2161-0444.1000135>
- Mousavi, S.S., Karami, A., Haghighi, T.M., Tumilaar, S.G., Fatimawali, Idroes, R., Mahmud, S., Celik, I., Ağagündüz, D., Tallei, T.E., 2021. In silico evaluation of Iranian medicinal plant phytoconstituents as inhibitors against main protease and the receptor-binding domain of SARS-CoV-2. *Molecules* 26(18), 5724. <https://doi.org/10.3390/molecules26185724>
- Nakagawa, K., Lokugamage, K., Makino, S., 2016. Viral and cellular mRNA translation in coronavirus-infected cells. *Advances in virus research* 96, 165-192. <https://doi.org/10.1016/bs.aivir.2016.08.001>
- Narayanan, B.A., Geoffroy, O., Willingham, M.C., Re, G.G., Nixon, D.W., 1999. p53/p21 (WAF1/CIP1) expression and its possible role in G1 arrest and apoptosis in ellagic acid treated cancer cells. *Cancer letters* 136(2), 215-221. [https://doi.org/10.1016/S0304-3835\(98\)00323-1](https://doi.org/10.1016/S0304-3835(98)00323-1)
- Ovesná, Z., Kozics, K., Slameňová, D., 2006. Protective effects of ursolic acid and oleanolic acid in leukemic cells. *Mutation Research/Fundamental and Molecular Mechanisms of Mutagenesis* 600(1-2), 131-137. <https://doi.org/10.1016/j.mrfmmm.2006.03.008>
- Park, S.W., Kwon, M.J., Yoo, J.Y., Choi, H.-J., Ahn, Y.-J., 2014. Antiviral activity and possible mode of action of ellagic acid identified in *Lagerstroemia speciosa* leaves toward human rhinoviruses. *BMC complementary and alternative medicine* 14, 1-8. <https://doi.org/10.1186/1472-6882-14-171>
- Petronelli, A., Pannitteri, G., Testa, U., 2009. Triterpenoids as new promising anticancer drugs. *Anti-cancer drugs* 20(10), 880-892. <https://doi.org/10.1097/CAD.0b013e328330fd90>
- Pizzato, M., Baraldi, C., Boscato Sopetto, G., Finozzi, D., Gentile, C., Gentile, M.D., Marconi, R., Paladino, D., Raoss, A., Riedmiller, I., 2022. SARS-CoV-2 and the host cell: a tale of interactions. *Frontiers in Virology* 1, 815388. <https://doi.org/10.3389/fviro.2021.815388>
- Pollier, J., Goossens, A., 2012. Oleanolic acid. *Phytochemistry* 77, 10-15. <https://doi.org/10.1016/j.phytochem.2011.12.022>
- Rehman, M.T., AlAjmi, M.F., Hussain, A., 2021. Natural compounds as inhibitors of SARS-CoV-2 main protease (3CLpro): A molecular docking and simulation approach to combat COVID-19. *Current pharmaceutical design* 27(33), 3577-3589. <https://doi.org/10.2174/1381612826999201116195851>
- Saleem, H.N., Batool, F., Mansoor, H.J., Shahzad-ul-Hussan, S., Saeed, M., 2019. Inhibition of dengue virus protease by eugenin, isobiflorin, and biflorin isolated from the flower buds of *Syzygium aromaticum*

- (Cloves). *Acs Omega* 4(1), 1525-1533. <https://doi.org/10.1021/acsomega.8b02861>
- Schwarz, S., Sauter, D., Wang, K., Zhang, R., Sun, B., Karioti, A., Bilia, A.R., Efferth, T., Schwarz, W., 2014. Kaempferol derivatives as antiviral drugs against the 3a channel protein of coronavirus. *Planta medica* 80(02/03), 177-182. <https://doi.org/10.1055/s-0033-1360277>
- Sharma, A., Tendulkar, A.V., Wangikar, P.P., 2011. Drug discovery against H1N1 virus (influenza A virus) via computational virtual screening approach. *Medicinal Chemistry Research* 20, 1445-1449. <https://doi.org/10.1007/s00044-010-9375-5>
- Shin, D., Mukherjee, R., Grewe, D., Bojkova, D., Baek, K., Bhattacharya, A., Schulz, L., Widera, M., Mehdi-pour, A.R., Tascher, G., 2020. Papain-like protease regulates SARS-CoV-2 viral spread and innate immunity. *Nature* 587(7835), 657-662. <https://doi.org/10.1038/s41586-020-2601-5>
- Singh, N.A., Kumar, P., Jyoti, Kumar, N., 2021. Spices and herbs: potential antiviral preventives and immunity boosters during COVID-19. *Phytotherapy Research* 35(5), 2745-2757. <https://doi.org/10.1002/ptr.7019>
- Somova, L., Shode, F., Ramnanan, P., Nadar, A., 2003. Antihypertensive, antiatherosclerotic and antioxidant activity of triterpenoids isolated from *Olea europaea*, subspecies *africana* leaves. *Journal of ethnopharmacology* 84(2-3), 299-305. [https://doi.org/10.1016/S0378-8741\(02\)00332-X](https://doi.org/10.1016/S0378-8741(02)00332-X)
- Sultana, N., Ata, A., 2008. Oleanolic acid and related derivatives as medicinally important compounds. *Journal of enzyme inhibition and medicinal chemistry* 23(6), 739-756. <https://doi.org/10.1080/14756360701633187>
- Tsai, Y., Cole, L.L., Davis, L.E., Lockwood, S.J., Simmons, V., Wild, G.C., 1985. Antiviral properties of garlic: in vitro effects on influenza B, herpes simplex and coxsackie viruses. *Planta medica* 51(05), 460-461. <https://doi.org/10.1055/s-2007-969553>
- ul Qamar, M.T., Alqahtani, S.M., Alamri, M.A., Chen, L.-L., 2020. Structural basis of SARS-CoV-2 3CLpro and anti-COVID-19 drug discovery from medicinal plants. *Journal of pharmaceutical analysis* 10(4), 313-319. <https://doi.org/10.1016/j.jpha.2020.03.009>
- Vicidomini, C., Roviello, V., Roviello, G.N., 2021. Molecular basis of the therapeutical potential of clove (*Syzygium aromaticum* L.) and clues to its anti-COVID-19 utility. *Molecules* 26(7), 1880. <https://doi.org/10.3390/molecules26071880>
- Vijayasteltar, L., Nair, G.G., Maliakel, B., Kuttan, R., Krishnakumar, I., 2016. Safety assessment of a standardized polyphenolic extract of clove buds: Subchronic toxicity and mutagenicity studies. *Toxicology reports* 3, 439-449. <https://doi.org/10.1016/j.toxrep.2016.04.001>
- Weber, N.D., Andersen, D.O., North, J.A., Murray, B.K., Lawson, L.D., Hughes, B.G., 1992. In vitro virucidal effects of *Allium sativum* (garlic) extract and compounds. *Planta medica* 58(05), 417-423. <https://doi.org/10.1055/s-2006-961504>
- Wong, N.A., Saier Jr, M.H., 2021. The SARS-coronavirus infection cycle: a survey of viral membrane proteins, their functional interactions and pathogenesis. *International journal of molecular sciences* 22(3), 1308. <https://doi.org/10.3390/ijms22031308>
- Yu, D., Sakurai, Y., Chen, C.-H., Chang, F.-R., Huang, L., Kashiwada, Y., Lee, K.-H., 2006. Anti-AIDS agents 69. Moronic acid and other triterpene derivatives as novel potent anti-HIV agents. *Journal of medicinal chemistry* 49(18), 5462-5469. <https://doi.org/10.1021/jm0601912>
- Zhang, D., Zhu, L., Wang, Y., Li, P., Gao, Y., 2022. Translational control of covid-19 and its therapeutic implication. *Frontiers in immunology* 13, 857490. <https://doi.org/10.3389/fimmu.2022.857490>
- Zhu, Y.-M., Shen, J.-K., Wang, H.-K., Cosentino, L.M., Lee, K.-H., 2001. Synthesis and anti-HIV activity of oleanolic acid derivatives. *Bioorganic & medicinal chemistry letters* 11(24), 3115-3118. [https://doi.org/10.1016/S0960-894X\(01\)00647-3](https://doi.org/10.1016/S0960-894X(01)00647-3)